Basic Study on Application of Discrete Element Method for Slope Failure Analysis

Y. Kawamura
JIP TechnoScience Corp., Japan

Y. Kobayashi
Nihon University, Japan

SUMMARY:
The discrete element method is characterized by its applicability for moving boundary condition. In this paper, as a basic study on application of discrete element method for slope failure analysis, effects of particle shape to the result of analyses are studied. To represent the irregular particle shape, some sphere particles are combined as a cluster. Tension forces are allowed to combine sphere particles and keep these relative positions, and it consequently makes behave the combined sphere particles as a unified object. The behaviour of a mass model that consists of the clusters is investigated by comparing the result of similar mass model consists of sphere particles. The result reveals the importance of particle shape on the behaviour of the mass model.

Keywords: Discrete element method, interaction, particle shape, particle cluster, inter locking

1. INTRODUCTION

In decades, disastrous slope failures were frequently reported while severe disaster events such as strong earthquakes and downpours. Many research projects have been organized to figure out its mechanism and developed countermeasures to prevent the disasters. Conventionally, important role of them is forecasting occurrence of slope failures; however, its aim is extending to quantitative estimation of extent of damage district recently because of spreading of the idea of the performance design. For the estimation, the deformation of slopes has to be predicted quantitatively. For this purpose, a method that adequately handles moving boundary problem is required, and various types of numerical methods have been studied. As one of them, discrete element method is quoted.

Discrete element method (DEM) is one of the methods based on mechanics of granular materials and applied for masses that are formed with granular materials. In DEM, the masses are numerically represented as a group of points, and each point is associated with a physical particle in the mass. Further, relationships among the particles are modelled by springs and dashpots that are respectively installed in normal and shear directions. DEM has been widely applied for various fields of engineering (Venugopal et al, 2001, Radziszewski, 1999), and especially, in case of civil engineering, it has been adopted for the analyses on element tests, slope failure and rock falls due to its applicability for moving boundary problems and easiness. (Cheng et al, 2003)

DEM often adopts sphere particle for the analysis to simplify its computational procedure. However, the use of sphere particle leads insufficient representation of interlocking between soil particles, and it may have significant influence on the result of analyses. To clarify the nature, the feature of DEM that takes the effect of particle shape into account is studied in this paper. For the consideration of particle shape in DEM, some sphere particles are combined and form a cluster to reproduce irregular shape of soil particles, and tension forces among the particles are introduced to keep relative position of each particle in the cluster. This method is applied for some examples and its feature is examined by comparing the result of analyses for models that are respectively formed by sphere and clustered particles.

2. INTRODUCTION OF DISCRETE ELEMENT METHOD

DEM models masses as group of computational points as illustrated in Fig. 2.1.

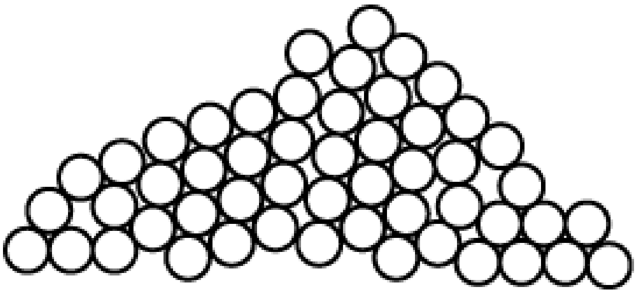

Figure 2.1 Representation of mass by DEM

The each computational point in the group is associated with a physical particle, and it is assumed that the behavior of the particle is governed by its body force and interaction force among particles. The governing equation of the particle is described as follows.

$$F = ma \tag{2.1}$$

This is the equation of motion, and F, m and a denote external and internal force, mass of the particle, and acceleration of the particle, respectively. The particles are modelled as rigid body and relationship between two particles are represented by springs and dashpots that are installed in normal and shear direction between the particles as illustrated in Fig. 2.2.

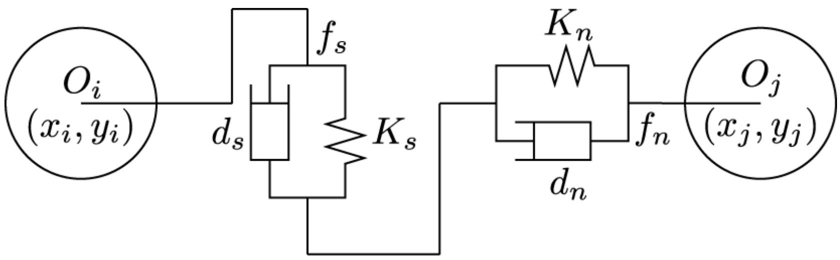

Figure 2.2 Springs and dashpots between two particles

Since F in Eqn. 2.1 includes interaction force between the two particles, Eqn. 2.1 is expanded as follows.

$$m\ddot{u} + \eta\dot{u} + Ku = 0 \tag{2.2}$$
$$I\ddot{\varphi} + \eta r^2\dot{\varphi} + Kr^2\varphi = 0 \tag{2.3}$$

in which, η is viscosity of dashpot, K is spring constant, I is moment of inertia, r is radius of particle, u is translation of particle and φ is rotation of particle, respectively. Since behavior of particles is coupling each other, Eqns. 2.2 and 2.3 are consequently coupled equation. For solving these equations, implicit time integration is quoted as a candidate of time integration to obtain the result precisely. However, the cost of it rapidly increases with increment of number of particles, and it leads difficulty of its application for practical problems. Hence, this equation of motion is explicitly integrated in time domain conventionally. Therefore the location, velocity and acceleration of each particle are obtained by assuming that the acceleration in current time step is estimated from the velocity and location in previous time step as described as follows.

$$m[\ddot{u}]_t + \eta[\dot{u}]_{t-\Delta t} + K[u]_{t-\Delta t} = 0 \tag{2.4}$$
$$m[\ddot{u}]_t = -\eta[\dot{u}]_{t-\Delta t} - \mathrm{K}[u]_{t-\Delta t} \tag{2.5}$$

For solving Eqn 2.5, contact of particles has to be evaluated to compute its interaction force. The contact of particles is evaluated from the distance between two particles as shown in Fig. 2.3.

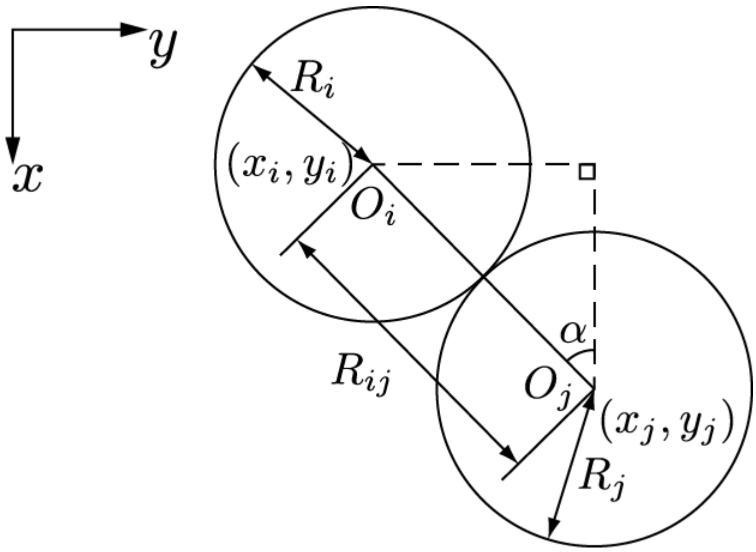

Figure 2.3 Evaluation of particle contact

As illustrated in Figure 2.3, the distance between two particles is computed as follows.

$$R_{ij} = \left\{\left(x_i - x_j\right)^2 + \left(y_i - y_j\right)^2\right\}^{\frac{1}{2}} \tag{2.6}$$

where x_i, y_i, x_j, y_j and R_{ij} denote x coordinate of particle i, y coordinate of particle i, x coordinate of particle j, y coordinate of particle j and distance between particle i and j, respectively. Then it is evaluated that two particles contact each other if following equation is fulfilled.

$$R_i + R_j \geq R_{ij} \tag{2.7}$$

For obtaining point of contact between particle i and j, α that is angle between line that connects center of particle i and j and x axis are calculated from following relationship.

$$\sin\alpha = -\left(y_i - y_j\right)/R_{ij} \tag{2.8}$$
$$\cos\alpha = -\left(x_i - x_j\right)/R_{ij} \tag{2.9}$$

Then the relative displacement between the two particles are obtained as follows

$$\Delta u_n = \left(\Delta u_i - \Delta u_j\right)\cos\alpha + \left(\Delta v_i - \Delta v_j\right)\sin\alpha \tag{2.10}$$
$$\Delta u_s = -\left(\Delta u_i - \Delta u_j\right)\sin\alpha + \left(\Delta v_i - \Delta v_j\right)\cos\alpha + \left(R_i\Delta\varphi_i + R_j\Delta\varphi_j\right) \tag{2.11}$$

in which, Δu_n, Δu_s, Δu_i, Δu_j, Δv_i, Δv_j, $\Delta\varphi_i$, $\Delta\varphi_j$, R_i and R_j are relative displacement in normal and shear direction, displacement of particle i and j in x direction, displacement of particle i and j in y direction, rotation of particle i and j and radius of particle i and j, respectively.

Interaction forces between two particles are described by using relative displacement and velocity in normal and shear direction since the two particles are connected by springs and dashpots in the two directions as illustrated in Fig. 2. 2. The interaction force in normal direction is described as follows.

$$\Delta e_n = \mathrm{K}_n\Delta u_n \tag{2.12}$$

$$\Delta d_n = \eta_n \frac{\Delta u_n}{\Delta t} \tag{2.13}$$
$$[e_n]_t = [e_n]_{t-\Delta t} + \Delta e_n \tag{2.14}$$
$$[d_n]_t = \Delta d_n \tag{2.15}$$
$$[f_n]_t = [e_n]_t + [d_n]_t \tag{2.16}$$

where, Δe_n, K_n, Δd_n, η_n, Δt, $[e_n]_{t-\Delta t}$, $[e_n]_t$ and $[f_n]_t$ are increment of the elastic interaction force, spring constant, increment of viscous force, coefficient of viscosity, time interval, elastic interaction force in previous step, elastic interaction force in current step and total interaction force in current step. It is note that compression force is positive in the interactive force in this paper. Furthermore, it is noteworthy that the negative interaction force in normal direction is cut off since generally tensional force is not considered in DEM.

In the meantime, the interaction force in shear direction is introduced as well

$$\Delta e_s = K_s \Delta u_s \tag{2.17}$$
$$[e_s]_t = [e_s]_{t-\Delta t} + \Delta e_s \tag{2.18}$$
$$\Delta d_s = \eta_s \frac{\Delta u_s}{\Delta t} \tag{2.19}$$
$$[d_s]_t = \Delta d_s \tag{2.20}$$
$$[f_s]_t = [e_s]_t + [d_s]_t \tag{2.21}$$

where, Δe_s, K_s, Δd_s, η_s, $[e_s]_{t-\Delta t}$, $[e_s]_t$ and $[f_s]_t$ are increment of the elastic interaction force, spring constant, increment of viscous force, coefficient of viscosity, elastic interaction force in previous step, elastic interaction force in current step and total interaction force in current step. It is noteworthy that the friction force generally has an upper limit that is given as Coulomb friction. Therefore, in this paper, the upper limit of the friction force is applied to the interaction force in shear direction.

Total forces to each particle are obtained by summing interaction, external and body force in each axis direction as follows.

$$[X_i] = \sum_j \{-[f_n]_t \cos\alpha + [f_s]_t \sin\alpha\} + \mathrm{mg} \tag{2.22}$$
$$[Y_i] = \sum_j \{-[f_n]_t \sin\alpha + [f_s]_t \cos\alpha\} \tag{2.23}$$
$$[M_i] = -R_i \sum_j \{[f_s]_t\} \tag{2.24}$$

in which, $[X_i]$, $[Y_i]$, $[M_i]$ and R_i denote total force in x direction, total force in y direction, total moment and radius of particle i, respectively. Since these forces forms total force to the particle i, the acceleration of particle i is obtained by dividing these forces by the mass or moment of inertia as follows

$$[\ddot{u}]_t = [X_i]/m \tag{2.25}$$
$$[\ddot{v}]_t = [Y_i]/m \tag{2.26}$$
$$[\ddot{\varphi}]_t = [M_i]/I \tag{2.27}$$

Velocity and location of particle i are computed explicitly from the acceleration of particles that are described in Eqns. 2.25 to 2.27. This procedure is applied for all of the particles, and behaviour of the mass formed by the particles is simulated.

For the procedures that are introduced above, the spring constant and coefficient of viscosity are necessary. Although many policies to determine them are proposed in previous research, the spring constant is obtained by the Hertz theory in this paper. According to the theory, the spring constant between two particles is shown as follows.

$$K = \frac{4a}{3} \times k^{-1} \tag{2.28}$$

The a and k are given as follows.

$$k = \left(\frac{1-\nu_i^2}{\mathrm{E}_i} + \frac{1-\nu_j^2}{\mathrm{E}_j}\right) \tag{2.29}$$

$$P = \frac{4}{3}\left[k^2 \times \left(\frac{1}{\mathrm{R}_i} + \frac{1}{\mathrm{R}_j}\right)\right]^{-\frac{1}{2}} \delta^{\frac{3}{2}} \tag{2.30}$$

$$a = \left[\frac{3}{4} k \times \left(\frac{1}{\mathrm{R}_i} + \frac{1}{\mathrm{R}_j}\right)^{-1} \times P\right]^{\frac{1}{3}} \tag{2.31}$$

where, ν_i, ν_j, E_i, E_j, δ and a are Poisons' ratio of particle i and j, Young's modulus of particle i and j, amount of overlap between particle i and j and contact radius as illustrated in Fig. 2.4.

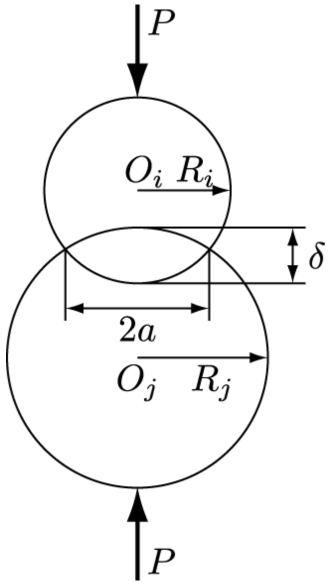

Figure 2.4 Brief diagram of assumption of Hertz Theory

Further, the coefficient of viscosity of the dashpot is set as follows.

$$\eta = 2\sqrt{m\mathrm{K}} \tag{2.32}$$

Eqn. 2.32 indicates that the coefficient of viscosity is defined to achieve critical damping if the two particles that are connected by the spring and dashpot form a vibration system of one degree of freedom. This damping stabilizes the system due to its energy dissipation.

3. CLUSTER OF SPHERE PARTICLES

The earth material is cluster of soil particles, and its stiffness and strength are influenced by interaction among the soil particles. Generally, the geometric configuration of soil particle is different if the material is different, and the difference would be a significant factor that changes nature of the interaction. This affects to the total behaviour of the masses modelled by DEM, and it is one of significant matter of the prediction of the model behaviour. To consider the influence of irregular particle shape, friction force has been conventionally adjusted to fit computed results to experimental results. However, this policy has limitation that the representation of interlocking among soil particles is insufficient. Hence, in this paper, the variation of particle shape is taken into account in DEM, and its feature is investigated.

The irregular shape of particles is represented by combining some sphere particles as illustrated in Fig. 3.1.

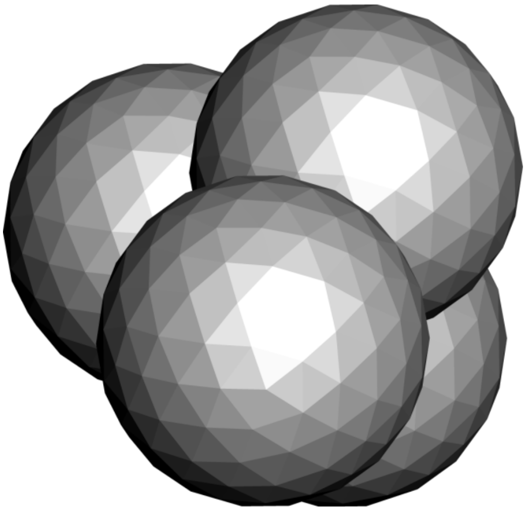

Figure 3.1 Cluster of sphere particles

The tension force is kept to retain relative position of each particle in the cluster, although the tension force is normally cut off in DEM.

4. EXAMPLE ANALYSIS

The influence of the irregular particle shape is investigated by some simple examples. Fig. 4.1 briefly introduces the example model.

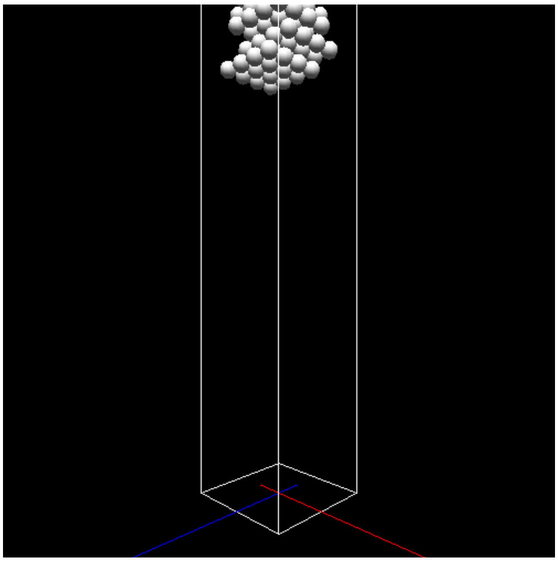

Figure 4.1 Initial setup of sphere particle model

In these examples, sphere particles or particle clusters that represents irregular particle shape are fallen from top of the model, and then stacked on the bottom of the model. After achieving stabilization in adequate time of analysis, the state of the models are adopted as initial states of the analyses. All of the walls on all side of the models are removed, and then analyses of failure of the mass formed by particles or clusters are demonstrated to investigate the effect of its shape. Fig. 4.2 illustrate initial state of the example analyses. The left figure in Fig. 4.2 shows the initial state of a case that sphere particles are adopted. This case is named Case1. Meanwhile, the right figure in Fig. 4.2 shows the initial state of another case that the particle clusters adopted to form the example model. This case is named Case2. According to these Figures, the dense of particle or clusters looks slightly different in these cases due to the effect of the particle shape. However, the height of the stacked mas is almost the same, and it is supposed that the initial configurations of the examples are sufficiently close.

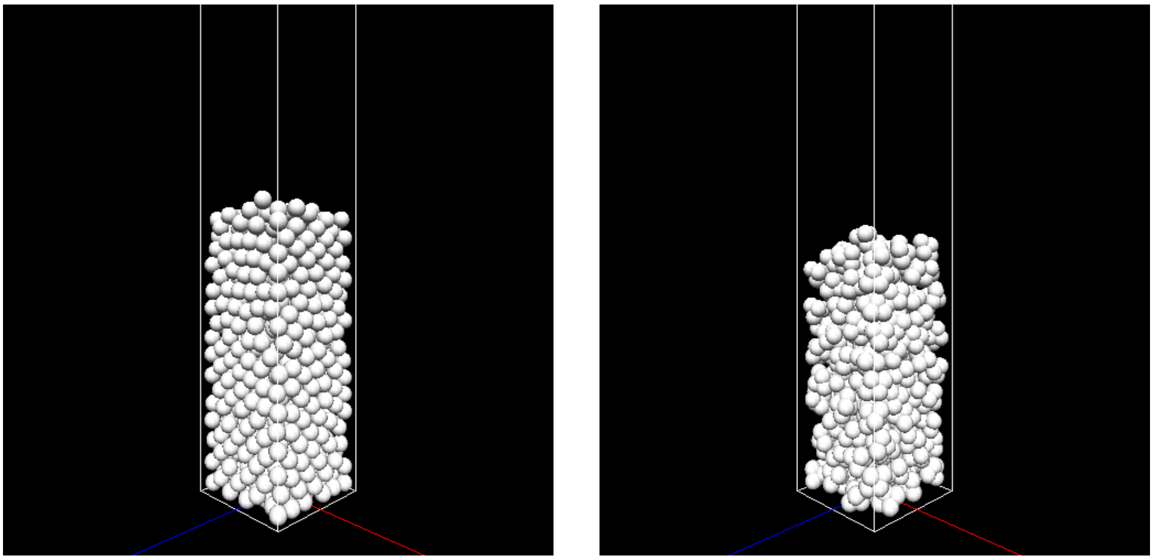

Figure 4.2. Initial state of sphere particle model (Left) and particle cluster model (Right)

Table 4.1 describes the material parameter for both cases. This is note that the material parameters are incompatible with real materials since these are determined only to check the influence of the particle shape and not intended to represents real phenomena. Further, the radius of each particle is fixed to 2.00 mm.

Table 4.1. Material Property

Time interval [s]	1/500000	Total analysis time [s]	240
Coefficient of friction	0.05	Mass of a particle [g]	0.064
Young’s modulus [Pa]	4.00E+6	Poisson’s ratio	0.28

Fig. 4.3 illustrates the transition of model configuration in Case1. According to the left figure of Fig. 4.3, it is seen that the model starts to fall down after removing all walls on all side and the sphere particles that forms the model spreads toward to outside of the wall. After sufficient elapsed time, the model proceeds to the equilibrium state. In this process, it is seen that the shape of the mass approaches to flat as illustrated in Fig. 4.3. In this analysis, the friction among the particles are taken into account to reproduce the effect of the interlocking of particles, however, it is shown that the effect is insufficient. Although the resultant shape of the mass is intended to be higher than the result of the analysis in its height, it is consequently more flat by tumble of the particles. This is caused by lack of interlocking of the sphere particles, and this tendency seems to be different from the behaviour of natural soil particles.

Fig. 4.4 illustrates the transition of model configuration in Case2. According to Fig. 4.4, the model spreads toward to outside of the wall as well in the beginning of failure of the mass. However, after a while, it is shown that the failure stops in the middle of the deformation, and resultant configuration of the mass is closer to the common deformation than Case1. This is caused by the effect of the shape of the particle cluster. The shape prevents the tumble of the particle and promotes engagement of particles in this case. This influence consequently constructs particle skeleton and suppress excess deformation of the mass. This result suggests that the consideration of the particle shape is significantly important to estimate the deformation of masses in DEM.

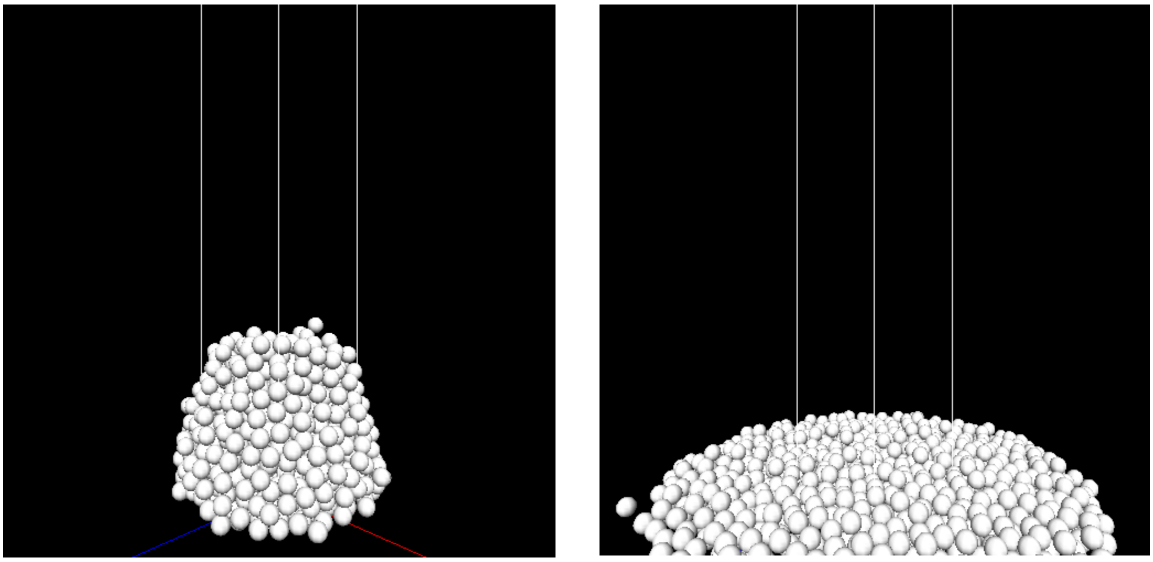

Figure 4.3 Transition of model configuration in Case 1

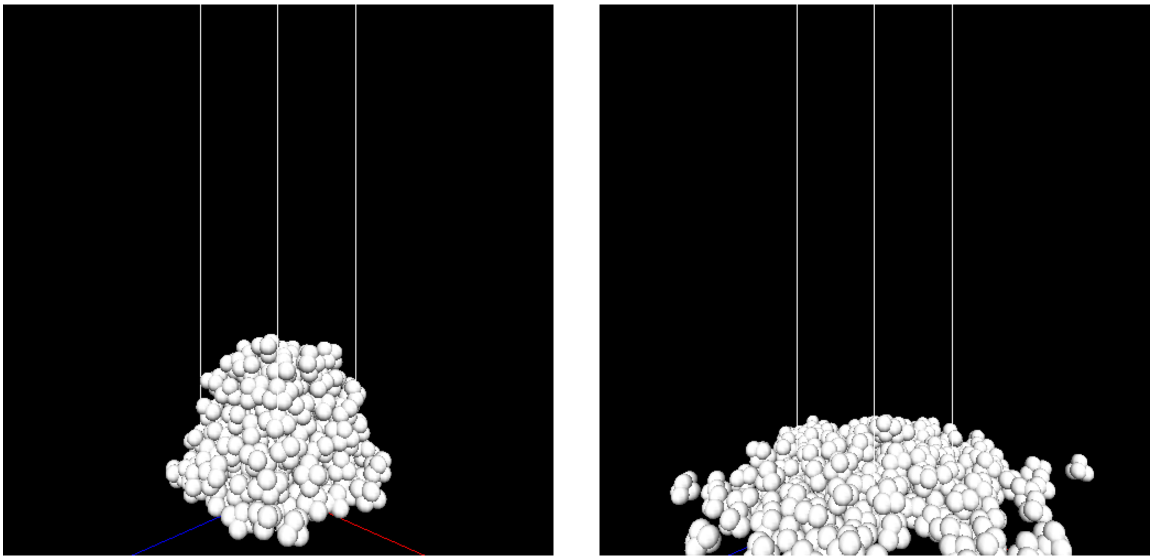

Figure4.4 Transition of model configuration in Case 2

Fig.4.5 illustrates the skeleton of particles that are formed by contacts of the particles or clusters after sufficient elapsed time in the analyses. In Fig. 4.5, lines imply the contacts of particles. According to the Fig. 4.5, it is shown that the connection is uniformly spread all over the mass in Case1. This tendency describes a fact that a particle is contacting with the other particle at many points, and the contact force is distributed to the points. This implies the interlocking of the particles is weak and particle skeleton is not constructed well in Case1. On the other hand, the number of contact points is smaller than Case1 in Case2 as illustrated in Fig. 4.5. This fact consequently leads that the contact force is relatively higher in Case2. This implies that the number of contact points is reduced since the particle cluster forms the skeleton by the interlocking.

Fig. 4.6 and Fig. 4.7 show comparison of time history of contact force of a particle that is located at the bottom of the mass in the initial setup. These figures also suggest that opportunities of particle contact are more frequent in sphere particle model than particle cluster model and the contact force is higher in case of particle cluster model. It is note that the tension force is found in Case2 since it is approved.

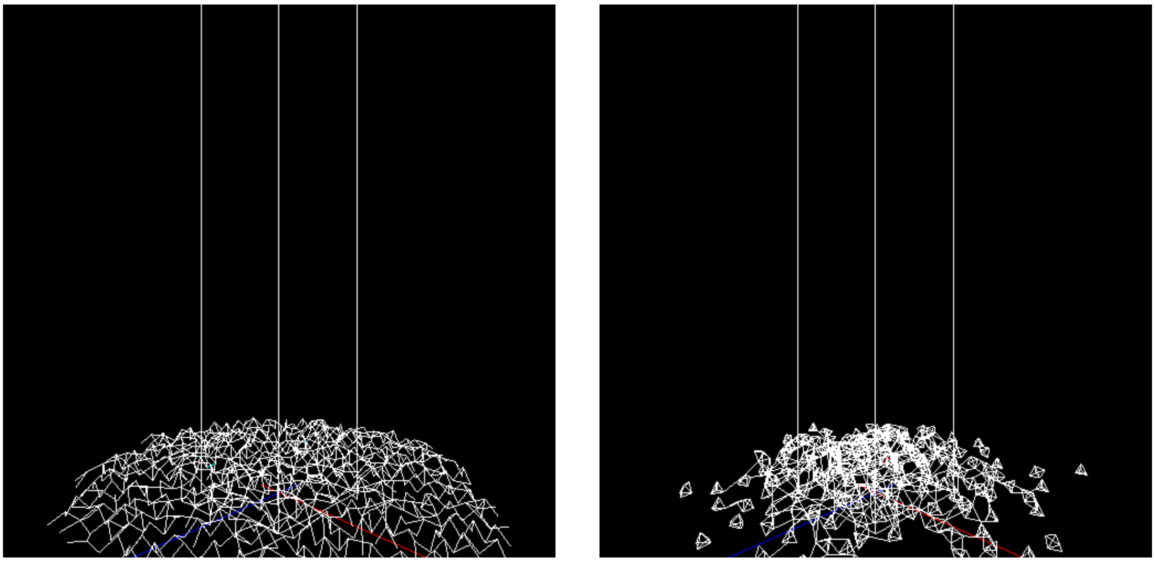

Figure 4.5 Particle Skeleton (Left Case1, Right Case2)

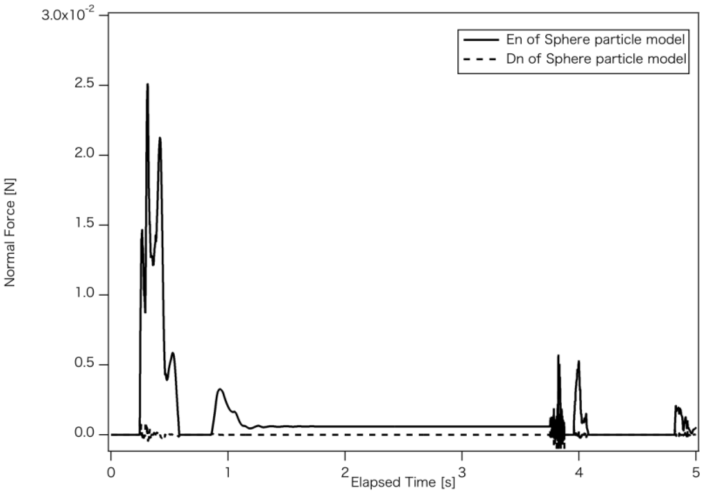

Figure 4.6 Time history of interaction force in normal direction at bottom of the sphere particle model

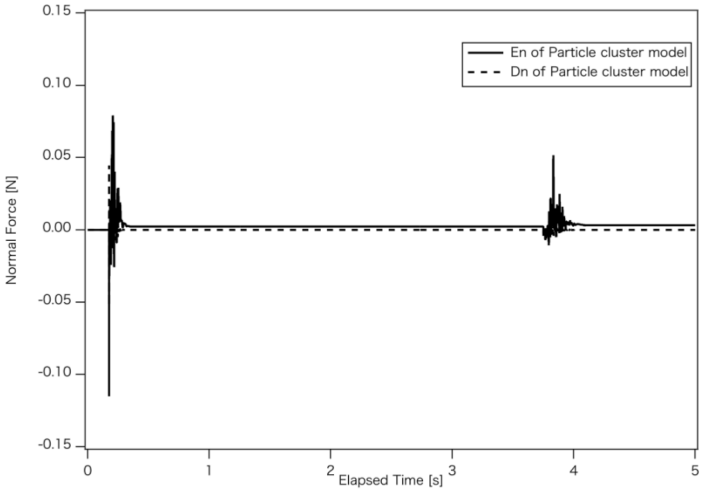

Figure 4.7 Time history of interaction force in normal direction at bottom of the particle cluster model

5. CONCLUDING REMARKS

In this paper, the effect of irregular particle shape on DEM analysis was studied. The irregular particle shape was represented by combining some sphere particles into a cluster, and the behaviour of masses that were formed by the sphere particles and particle clusters were investigated by comparing the results. The result of the investigations shows the behaviour of the models clearly depends on the particle shape, and it suggests the importance of consideration of the interlocking for the estimation of the model behaviour.

ACKNOWLEDGEMENT
This work was supported by Grants –in-Aid for Scientific Research.

REFERENCES

Cheng, Y. P., Nakata, Y and Bolton, M. D. (2003). Distinct element simulation of crushable soil. *Geotechnique* **53:7**,633-641.

Radziszewski, P. (1999). Comparing Three DEM Charge Motion Models. *Minerals Engineering* **12:12**,1501-1520.

Venugopal, R. and Rajamani, R. K. (2001). 3D simulation of charge motion in tumbling mills by the discrete element method. *Powder Technology* **115**,157-166.